Classical Dual-Inverted-Pendulum Control

Kent H. Lundberg   James K. Roberge

Department of Electrical Engineering and Computer Science

Massachusetts Institute of Technology, Cambridge, MA 02139

email: klund(at)mit.edu

Abstract— A cart with two independent inverted pendula, called a dual-inverted-pendulum system, is analyzed and compared to the single-inverted-pendulum system using classical linear methods. Using only the angles of the pendula and the position of the cart, a classical controller is designed that stabilizes the pendula in the inverted position with the cart at the center of the track. Simulations of the transient response to initial conditions are presented. Intuitive reasoning and an insightful approach to the control design are major emphases of this effort.

I. INTRODUCTION

The feedback stabilization of a single-inverted-pendulum system, shown in Figure 1, is a favorite lecture demonstration of students in control subjects, and is well covered in the literature [1], [2], [3]. The single-inverted-pendulum system has an elegant classical controller, requiring only easily measured inputs: the angle of the pendulum with respect to vertical and the position of the cart.

The position of the cart must be measured to keep the system from driving off the end of the track. The primary difficulty in the design of the classical controller for the inverted-pendulum system is maintaining the controllability of the cart-position mode.
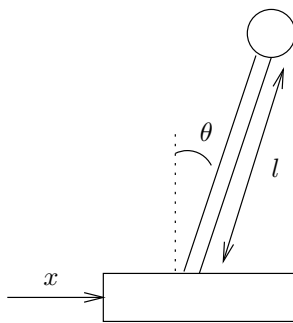

Fig. 1.   Geometry of the single-inverted-pendulum system (driving servomechanism not shown)

A cart with two independent inverted pendula [4], [5], here called a "dual-inverted-pendulum system," is shown in Figure 2. The position of the cart x is driven by a servomechanism. The angles of the pendulum with respect to vertical are θ_B for the big pendulum and θ_L for the little pendulum.

In the following sections, a compensator that stabilizes the pendula in the inverted position and keeps the cart near the
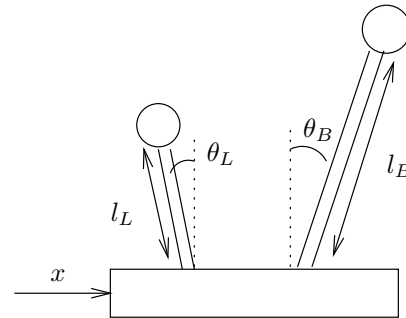

Fig. 2.   Geometry of the dual-inverted-pendulum system (driving servomechanism not shown)

center of the track is devised using only measurements of the pendula angle and the position of the cart.

II. INVERTED-PENDULUM MODEL

Following the development by Siebert [6], the transfer function for the inverted-pendulum system is written in terms of the cart position. Consider the inverted-pendulum system in Figure 1. At a pendulum angle of θ from vertical, gravity produces an angular acceleration equal to

$$\ddot{\theta}_g = (g/l) \sin \theta$$

and a cart acceleration of $\ddot{x}$ produces an angular acceleration of

$$\ddot{\theta}_x = -(\ddot{x}/l) \cos \theta.$$

Writing these accelerations as an equation of motion, linearizing it, and taking its Laplace transform produces the plant transfer function $G(s)$, as follows:

$$\ddot{\theta} = \ddot{\theta}_g + \ddot{\theta}_x = (g/l) \sin \theta - (\ddot{x}/l) \cos \theta$$

$$l\ddot{\theta} - g\theta = -\ddot{x}$$

$$G(s) = \frac{\Theta(s)}{X(s)} = \frac{-s^2}{ls^2 - g} = \frac{-s^2/g}{(\tau s + 1)(\tau s - 1)}$$

where the time constant τ is defined as $\tau = \sqrt{l/g}$. This transfer function has a pole in the right half-plane, which is consistent with our intuitive expectation of instability.
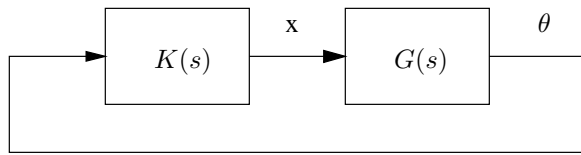
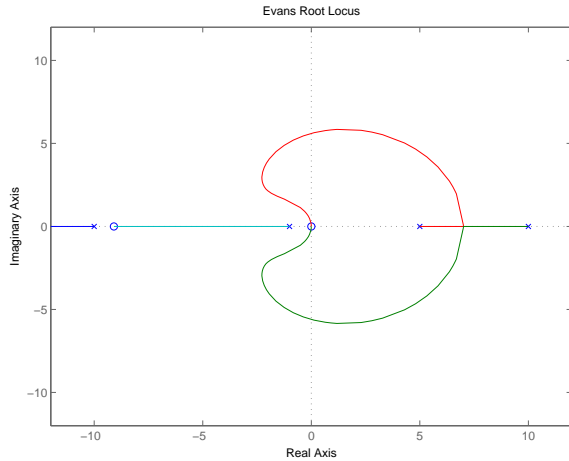Fig. 3.   Block diagram of the inverted-pendulum loop

Fig. 4.   Root locus of the inverted-pendulum-system loop with unstable compensator

III. SINGLE-INVERTED-PENDULUM STABILIZATION

The stabilization of the single-inverted-pendulum system is accomplished by driving the cart position based on the pendulum angle, as shown in the system block diagram in Figure 3.

The difficulty in stabilizing the inverted-pendulum system derives from the right half-plane pole in conjunction with the zeros at the origin. Canceling the zeros at the origin makes the cart position uncontrollable. In order to stabilize the system, the compensator must include a right half-plane pole, as explained below.

For example, with a pendulum length of $l = 9.8$ cm and acceleration due to gravity of $g = 9.8$ m/s^2, the pendulum transfer function is

$$G(s) = \frac{-s^2/g}{(0.1s + 1)(0.1s - 1)}$$

One possible stabilizing compensator is

$$K(s) = \frac{K(0.11s + 1)}{(s + 1)(0.2s - 1)}$$

as shown in the root locus in Figure 4.

The right half-plane pole in the compensator causes the root-locus branches in the right half-plane to break away from the real axis and travel into the left half-plane. Without the unstable pole in the compensator, the zeros at the origin would prevent the root-locus branch for the right half-plane pole from crossing the imaginary axis.

Intuitively, the unstable pole in the compensator is explained by the need for position feedback around the driving servomechanism. The cart position can be stabilized by adding
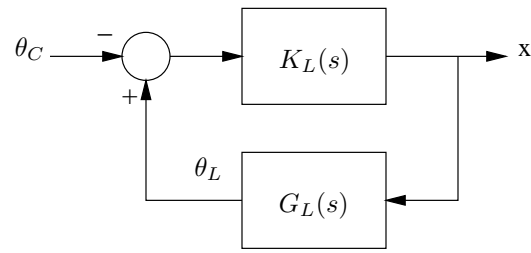
an offset to the angle measurement that is proportional to cart position. This feedback has the effect of always "leaning" the pendulum toward the center of the track, which prevents cart drift. This positive feedback pushes one of the motor poles into the right half-plane, as is shown in Figure 4.

IV. DUAL-INVERTED-PENDULUM CONTROL STRATEGY

The stabilizing control for the dual-inverted-pendulum system is developed using an approach similar to the single-inverted-pendulum system.

Conceptually, in order to stabilize this system, the controller must catch the little pendulum (because it's going to fall over first) and then catch the big pendulum. If the little pendulum is pointed in the same direction as the big pendulum, but at a larger angle, then the cart must move such as to catch both pendula. The only possible equilibrium for the system is with both pendula upright.

Obviously, the system cannot be stabilized if the pendula are identical in length. If the pendula are identical then they are affected equally by the motion of the cart. For example, if they are falling in opposite directions, any attempt to catch the pendulum falling to the left makes the pendulum falling to the right worse by the same amount. It is this property that makes the dual-inverted-pendulum system harder to stabilize than the articulated-inverted-pendulum system (often called the "double-inverted-pendulum system").

To implement the above control strategy, a minor loop is closed around the little pendulum that drives the cart position to regulate the little-pendulum angle θ_L. The little-pendulum angle is commanded to lean in the direction that the cart needs to travel, as shown in the block diagram of the minor loop in Figure 5. $G_L(s)$ is the little-pendulum transfer function, and $K_L(s)$ is the minor-loop compensator. Note that the block diagram is drawn with positive feedback since $G_L(s)$ includes a negative sign.

The transfer function from our command angle θ_C to the cart position x is

$$H_L(s) = \frac{X(s)}{\Theta_C(s)} = \frac{-K_L(s)}{1 - K_L(s)G_L(s)}$$

To control the angle of the big pendulum, the cart is driven via the minor-loop input θ_C based on the angle of the big pendulum with respect to vertical, θ_B. The control strategy is to make the minor-loop command some function of the big-pendulum angle, like $\theta_C = k_C\theta_B$. Thus, a compensator $K_C(s)$
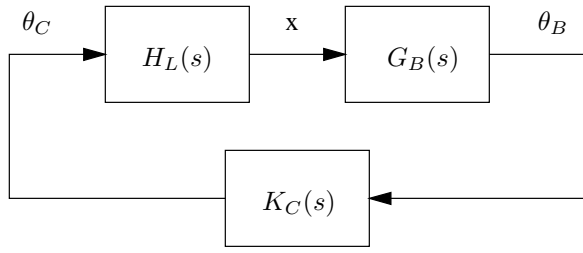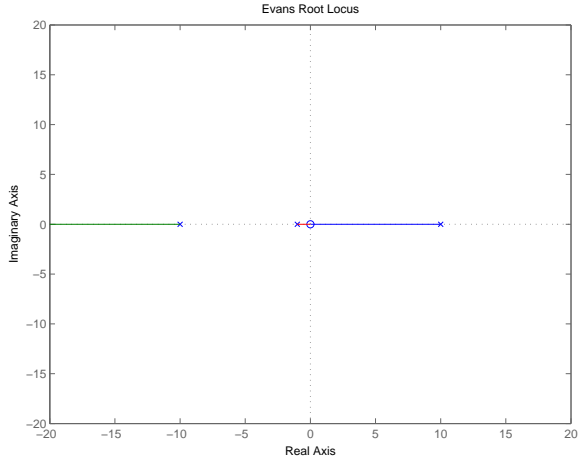
Fig. 6. Block diagram of the major loop

Fig. 7. Root locus of the minor-loop transfer function $L_m(s) = K_L(s)G_L(s)$

is designed, and the loop is closed from $\Theta_C(s)$ to $\Theta_B(s)$, as shown in the block diagram of the major loop in Figure 6.

V. LOOP DESIGN AND STABILIZATION

The linearized transfer function relating the angle of the little pendulum with respect to vertical θ_L to the position of the cart x is

$$G_L(s) = \frac{\Theta_L(s)}{X(s)} = \frac{-s^2/g}{(\tau_L s + 1)(\tau_L s - 1)}$$

where g is the acceleration due to gravity and the time constant is $\tau_L = \sqrt{l_L/g}$.

By analogy to the single-inverted-pendulum system, a compensator for the minor loop is chosen to leave one of the closed-loop minor-loop poles in the right half-plane. For a little-pendulum length of $l_L = 9.8$ cm, such a compensator is
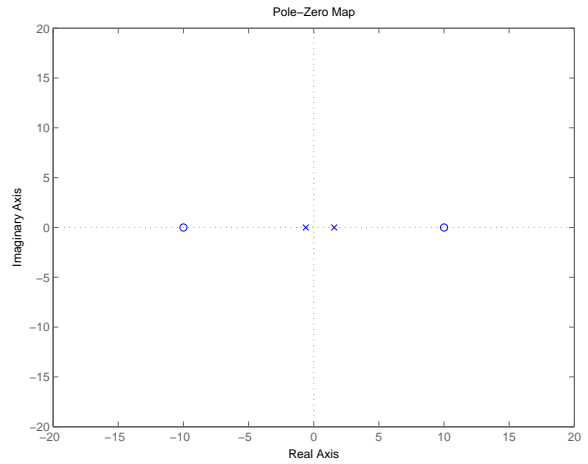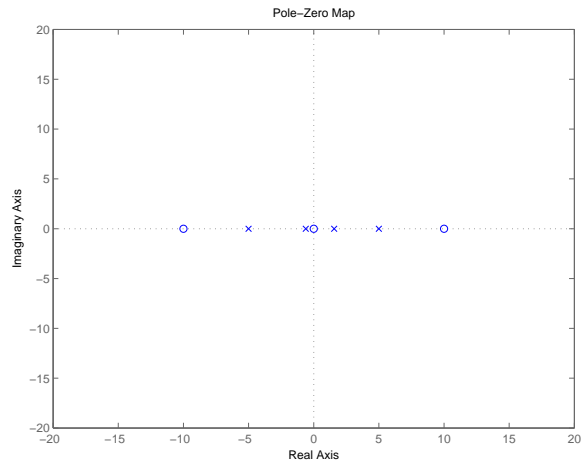
$$K_L(s) = \frac{10}{s + 1}$$

as shown in the root locus of the minor-loop transfer function

$$L_m(s) = K_L(s)G_L(s)$$

shown in Figure 7.

The minor-loop transfer function is

$$H_L(s) = \frac{X(s)}{\Theta_C(s)} = \frac{-K_L(s)}{1 - K_L(s)G_L(s)}$$

Fig. 8. Pole-zero plot of the transfer function $H_L(s)$ (closed minor loop)

Fig. 9. Pole-zero plot of the major-loop transfer function $L(s) = K_C(s)H_L(s)G_B(s)$

For the above $G_L(s)$ and $K_L(s)$, the pole-zero plot of $H_L(s)$ is shown in Figure 8.

The transfer function for the big pendulum is

$$G_B(s) = \frac{\Theta_B(s)}{X(s)} = \frac{-s^2/g}{(\tau_B s + 1)(\tau_B s - 1)}$$

where $\tau_B = \sqrt{l_B/g}$. With a big pendulum length four times longer than the little pendulum ($l_B = 4l_L$), the pole-zero plot of the major loop transfer function

$$L(s) = K_C(s)H_L(s)G_B(s)$$

is shown in Figure 9.

The pole-zero plot in Figure 9 shows two poles in the right half-plane, one from the minor loop and one from the big pendulum, as desired. Closing the major loop with a little bit of lead compensation

$$K_C(s) = k_C \left(\frac{\tau_B s + 1}{\tau_L s + 1} \right)$$

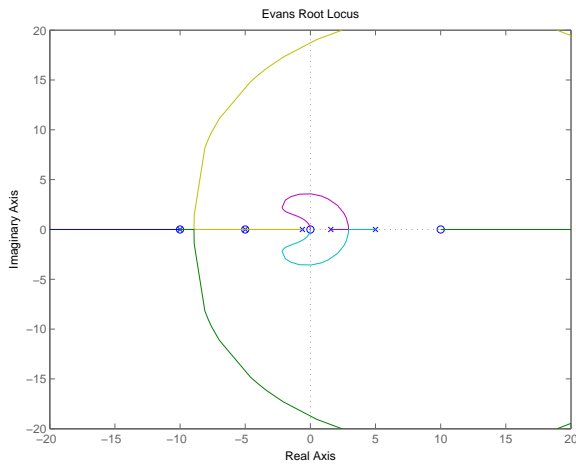produces the root-locus plot shown in Figure 10.

Fig. 10. Root locus of the major-loop transfer function $L(s) = K_C(s)H_L(s)G_B(s)$
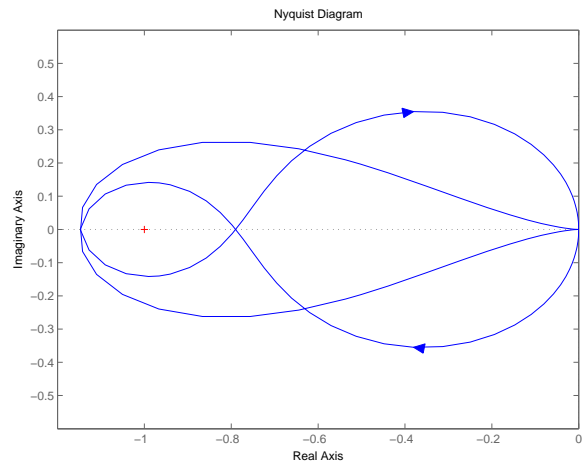

Fig. 12. Nyquist plot of the major-loop transfer function $L(s) = K_C(s)H_L(s)G_B(s)$ for $k_C = 1.5$
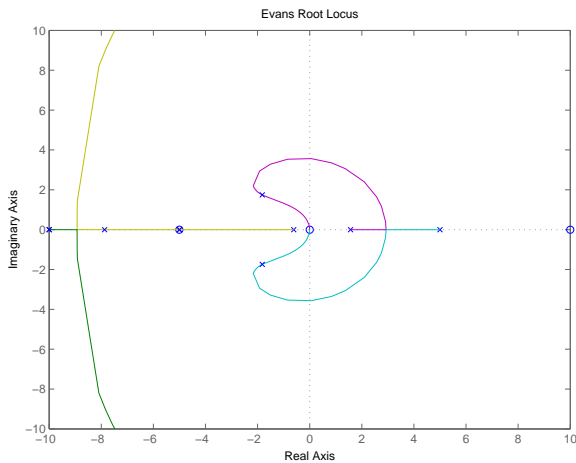

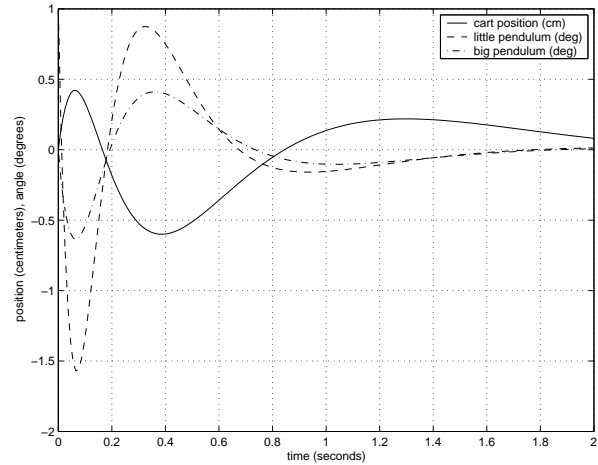Fig. 11. Root locus of the major loop with locations of closed-loop poles for $k_C = 1.5$

Fig. 13. Simulation of system for initial non-zero little-pendulum angle

Choosing $k_C = 1.5$ pushes the closed-loop poles of the major loop deep into the left half-plane, as shown on the root-locus plot in Figure 11. Note that this gain corresponds to driving the little-pendulum angle to 1.5 times the big-pendulum angle. This gain results in pole locations that provide acceptable transient behavior.

A Nyquist diagram of the major loop, as shown in Figure 12, shows that the system is stable as designed for $k_C = 1.5$. The two negative encirclements of the -1 point guarantee stability since the open-loop system starts with two poles in the right half-plane.

However, the Nyquist plot also shows that there is not much phase margin, so the system will likely go unstable if additional low-pass dynamics are added to the loop.

VI. SIMULATIONS

The system described in the previous section was simulated in Simulink [7] for three different initial conditions corre-

sponding to the three states of the system: little-pendulum angle, big-pendulum angle, and cart position.

A. Initial Little-Pendulum Angle

The system was simulated for the little pendulum initially leaning by one degree, with the big pendulum vertical and the cart centered on the track. The transient response to this initial condition is shown in Figure 13.

The transient deviations in angle and position make sense. In order to recover from an initial angle in the little pendulum, the cart must move to get both pendula pointing in the same direction. Only then can the cart move to make both pendula vertical.

B. Initial Big-Pendulum Angle

The system was simulated for the big pendulum initially leaning by one degree, with the little pendulum vertical and the cart centered on the track. The transient response to this initial condition is shown in Figure 14.
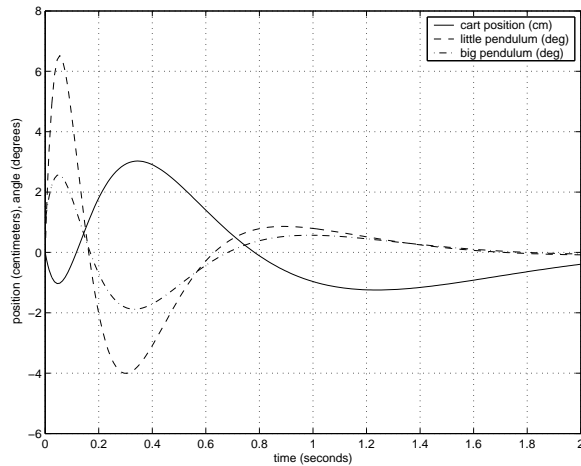
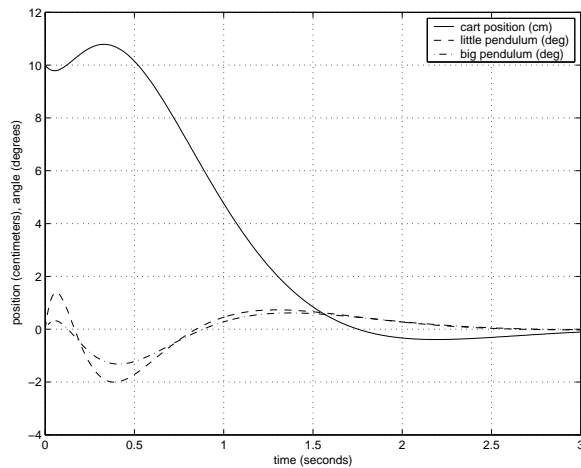Fig. 14.   Simulation of system for initial non-zero big-pendulum angle

Fig. 15.   Simulation of system for initial non-zero cart position

Again, the transient deviations in angle and position make sense, despite their larger amplitude. Note the system has to "work harder" to correct a deviation in the big pendulum than to correct a deviation in the little pendulum. In order to recover from an initial angle in the big pendulum, the cart must initially move in the direction to make the deviation worse, so both pendula are pointing in the same direction. This motion more than doubles the big pendulum angle, and creates a large transient deviation of the little pendulum. Once both pendula are leaning in the same direction (with the little pendulum leaning more), the cart moves back to correct both angles.

C. Initial Cart Position

The system was simulated for an initial cart position of ten centimeters, with the pendula vertical. The transient response to this initial condition is shown in Figure 15.

The complicated initial behavior of the cart can be readily explained. To move the cart to the left, the system must point the big pendulum to the left. To point the big pendulum to

the left, the little pendulum must first be pointed to the right. Therefore

1) The cart moves slightly to the left to point the little pendulum to the right
2) The cart moves to the right to point both pendula to the left
3) The cart moves smoothly to the left, catching both pendula and traveling the necessary distance

Intuitively, this behavior is correct. When balancing a vertical ruler in your hand, to move the ruler to the left, you must first move your hand sharply to the right, pointing the ruler to the left, so that when you catch the ruler, you have moved both your hand and ruler to the left.

VII. Conclusion

A logical extension to the classical controller for the single-inverted-pendulum system has been shown for the dual-inverted-pendulum system. This controller is simpler than the modern control result [8]. It is the result of an intuitive approach to the problem, and is easily understood.

Appendix
Limit on Phase Margin

The obtainable system phase margin can be estimated by ignoring the controllability of the cart position and designing a minimal compensator. Starting with the transfer function of the little pendulum

$$G_L(s) = \frac{\Theta_L(s)}{X(s)} = \frac{-s^2/g}{(\tau_L s + 1)(\tau_L s - 1)}$$

The minor loop can be stabilized by making x an appropriate function of θ_L. A simple choice for this compensator (which ignores the position mode) is

$$K_L(s) = \frac{k_L g(\tau_L s + 1)}{s^2}.$$

The system, shown in the block diagram of Figure 5, is stable for any $k_L > 1$. The transfer function for the closed minor loop, from command to cart position is

$$H_L(s) = \frac{X(s)}{\Theta_C(s)} = \frac{-K_L(s)}{1 - K_L(s)G_L(s)}$$

$$H_L(s) = -\frac{g(\tau_L s + 1)(\tau_L s - 1)}{s^2 \left(\frac{\tau_L s}{k_L} + 1 - \frac{1}{k_L}\right)}$$

In the limiting case of making the compensator gain k_L very large, the dynamics of the real axis pole are instantaneous, thus

$$H_L(s) = \frac{X(s)}{\Theta_C(s)} \approx -\frac{g(\tau_L s + 1)(\tau_L s - 1)}{s^2}$$

The transfer function of the big pendulum is

$$G_B(s) = \frac{\Theta_B(s)}{X(s)} = \frac{-s^2/g}{(\tau_B s + 1)(\tau_B s - 1)}$$

thus the transfer function of the major loop, shown in the block diagram of Figure 6, is

$$L(s) = K_C(s) H_L(s) G_B(s)$$

$$L(s) = K_C(s) \frac{(\tau_L s + 1)(\tau_L s - 1)}{(\tau_B s + 1)(\tau_B s - 1)}$$

One possible compensation technique for the major loop is to pick a $K_C(s)$ that cancels all of the left half-plane dynamics of the plant. This compensator is

$$K_C(s) = k_B \frac{(\tau_B s + 1)}{(\tau_L s + 1)}$$

thus, the loop transfer function of the major loop becomes

$$L(s) = k_B \frac{(\tau_L s - 1)}{(\tau_B s - 1)}$$

To achieve the most stable performance, the loop must crossover at $\omega_c = 1/\sqrt{\tau_L \tau_B}$ with $k_B = \sqrt{\tau_B/\tau_L}$. This system has a phase margin

$$\phi_M = \arcsin\left(\frac{\alpha - 1}{\alpha + 1}\right)$$

where $\alpha = \tau_B/\tau_L$. This equation is similar to the maximum obtainable phase increase from the lead compensator [9].

This development suggests that the stability of the system is improved if the ratio of the pendula lengths is increased. This result makes intuitive sense, because the system is obviously uncontrollable if the lengths are the same. However, it is inadvisable to increase the ratio without bound. Our choice for the major-loop compensator

$$K_C(s) = k_B \frac{(\tau_B s + 1)}{(\tau_L s + 1)}$$

has high-frequency gain proportional to the square root of the length ratio. Increasing the high-frequency gain of $K_C(s)$ increases the amplitude of the transient deviations of the little-pendulum angle. As can be seen from the simulation in Figure 14, for an initial big-pendulum angle of one degree, the transient deviation of the little-pendulum angle already approaches seven degrees. Increasing the length ratio will make the amplitude of this transient larger, possibly violating our assumption that $\sin\theta = \theta$.

REFERENCES

[1] James K. Roberge. The mechanical seal. Bachelor's thesis, Massachusetts Institute of Technology, May 1960.

[2] Richard C. Dorf. *Modern Control Systems*, pages 276–279. Addison-Wesley, Reading, Massachusetts, 1967.

[3] Katsuhiko Ogata. *Modern Control Engineering*, pages 277–279. Prentice-Hall, Englewood Cliffs, New Jersey, 1970.

[4] Donald T. Higdon and Robert H. Cannon, Jr. On the control of unstable multiple-output mechanical systems. ASME Publication 63-WA-148, American Society of Mechanical Engineers, New York, 1963.

[5] J. G. Truxal. State models, transfer functions, and simulation. Monograph 8, Discrete Systems Concept Project, 30 April 1965.

[6] William McC. Siebert. *Circuits, Signals, and Systems*, pages 177–182. MIT Press, Cambridge, Massachusetts, 1986.

[7] The MathWorks Inc. *Using Simulink Version 5*. Natick, Massachusetts, 2002.

[8] Lara C. Phillips. Control of a dual inverted pendulum system using linear-quadratic and H-infinity methods. Master's thesis, Massachusetts Institute of Technology, September 1994.

[9] James K. Roberge. *Operational Amplifiers: Theory and Practice*, page 173. Wiley, New York, 1975.